

From Shadows to Safety: Occlusion Tracking and Risk Mitigation for Urban Autonomous Driving

Korbinian Moller, Luis Schwarzmeier, Johannes Betz

Abstract—Autonomous vehicles (AVs) must navigate dynamic urban environments where occlusions and perception limitations introduce significant uncertainties. This research builds upon and extends existing approaches in risk-aware motion planning and occlusion tracking to address these challenges. While prior studies have developed individual methods for occlusion tracking and risk assessment, a comprehensive method integrating these techniques has not been fully explored. We, therefore, enhance a phantom agent-centric model by incorporating sequential reasoning to track occluded areas and predict potential hazards. Our model enables realistic scenario representation and context-aware risk evaluation by modeling diverse phantom agents, each with distinct behavior profiles. Simulations demonstrate that the proposed approach improves situational awareness and balances proactive safety with efficient traffic flow. While these results underline the potential of our method, validation in real-world scenarios is necessary to confirm its feasibility and generalizability. By utilizing and advancing established methodologies, this work contributes to safer and more reliable AV planning in complex urban environments. To support further research, our method is available as open-source software at <https://github.com/TUM-AVS/OcclusionAwareMotionPlanning>.

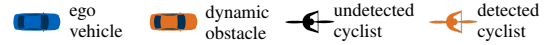
Index Terms—Autonomous Driving, Motion Planning, Safety, Occlusion Awareness, Vulnerable Road User

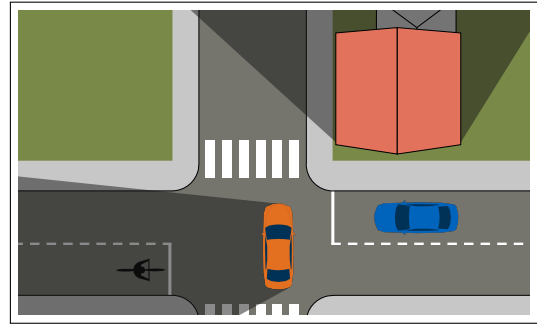
I. INTRODUCTION

Autonomous vehicles (AVs) hold the potential to revolutionize transportation by reducing accidents, enhancing mobility, and improving traffic efficiency [1]. However, their safe deployment in dynamic urban environments remains a considerable challenge, particularly when navigating scenarios involving vulnerable road users (VRUs) such as pedestrians and cyclists. Despite significant advancements, perception systems in AVs are inherently limited by constraints such as sensor range, field of view, and occlusions caused by static obstacles (e.g., parked vehicles or buildings) and dynamic objects (e.g., moving vehicles) [2]. These limitations result in hidden areas within the environment, introducing uncertainties that have been shown to contribute significantly to crashes [3].

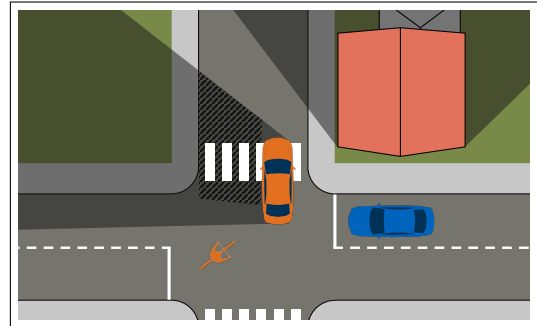
To ensure safe navigation despite these perception constraints, AVs must incorporate methods that compensate for limited perception capabilities. This involves dynamically assessing occluded areas and identifying potential hazards to enhance situational awareness and mitigate risks associated with occluded road users. By doing so, AVs can effectively balance proactive safety measures with efficient traffic flow.

K. Moller, L. Schwarzmeier and J. Betz are with the Professorship of Autonomous Vehicle Systems, TUM School of Engineering and Design, Technical University of Munich, 85748 Garching, Germany; Munich Institute of Robotics and Machine Intelligence (MIRMI).





(a) The cyclist is located in an occluded area and is not yet visible to the ego vehicle (EV).



(b) The cyclist emerges from the occluded area, becoming visible to the EV. The hatched region indicates an area where no objects can be present, as it was previously visible to the EV.

Fig. 1. Illustration of an intersection scenario emphasizing the importance of occlusion-aware planning.

Figure 1 illustrates a typical scenario where a cyclist emerges from an occluded area, underscoring the critical importance of occlusion-aware planning.

This paper addresses these challenges by proposing a motion planning algorithm that integrates and extends existing risk- and occlusion-aware motion planning approaches. Central to this approach is the enhancement of a phantom agent-centric model [4] to systematically track occluded areas to identify potential spawn points for occluded traffic participants. Sequential reasoning [5], [6] is employed as part of this tracking process, dynamically assessing which portions of the occluded area could realistically be reached by hidden agents based on their potential paths and speeds. This integration ensures that only relevant phantom agents (PAs) are considered in the planning process, reducing unnecessary computational overhead while focusing on real risks [4]. The

proposed method introduces diverse PA types, representing vehicles, pedestrians, and cyclists, each characterized by distinct behavior profiles. This diversity enables the planner to account for a wide range of potential actions and interactions. In conclusion, our proposed occlusion-aware motion planner presents four main contributions:

- 1) **A combination of agent-centric modeling and sequential reasoning:** This work integrates occlusion tracking with sequential reasoning to dynamically evaluate reachable areas in occluded zones. By focusing on PAs in relevant areas, only those traffic participants that pose a realistic risk are considered.
- 2) **A diverse PA framework for behavior modeling:** Our method introduces different PA types with various behavior profiles. This enables the representation of a wide range of possible actions, capturing diverse and realistic agent behaviors.
- 3) **Comprehensive simulation analysis:** Extensive simulations are conducted to evaluate the proposed approach in real-world-inspired scenarios. These analyses demonstrate the effectiveness of our method in improving occlusion awareness.
- 4) **Open-source software:** The occlusion-aware motion planner, including occlusion tracking methods and PA models, is published as open-source software.

II. RELATED WORK

The challenge of navigating environments with occluded obstacles has prompted a variety of approaches in autonomous driving research, each addressing different aspects of the problem.

One class of solutions employs Partially Observable Markov Decision Processes (POMDPs) to model the uncertainties associated with occluded areas. These methods reason about hidden traffic participants based on their potential trajectories and interactions [7], [8]. While POMDP-based approaches provide robust theoretical frameworks, their practical application often involves high computational complexity, limiting real-time feasibility.

Another strategy involves reachable sets, which predict the possible positions and velocities of occluded road users based on formalized traffic rules and motion models [9], [10]. These approaches have demonstrated versatility across various traffic scenarios, including urban intersections and autonomous parking maneuvers [11].

Several studies aim to mitigate occlusion risks by increasing the visible area. For instance, lateral position adjustments can expand sensor coverage, enabling AVs to detect otherwise occluded road users. Cost functions that prioritize visibility in trajectory planning foster collision avoidance [12], [13]. Similarly, infrastructure-based enhancements, such as roadside units (RSUs), extend the vehicle’s perception range by integrating local and external sensors [14]. In [15] the authors leveraged Vehicle-to-Everything (V2X) technology to improve visibility through sequential reasoning, demonstrating potential for urban environments. Despite these advancements, such methods depend on the availability of

external infrastructure, which is often not feasible in current real-world scenarios.

In [16], the authors propose a Dynamic Bayesian Network with Markov chains to tackle occlusions. By generating multimodal predictions and evaluating these in realistic use cases, the framework advances occlusion-aware planning.

Previous research has also explored methods to address agents that temporarily disappear. Pang et al. [17] introduced a motion prediction framework that propagates past positions of occluded agents using multi-modal trajectory predictions and differentiable filters to ensure temporal coherence.

Another line of research models occluded road users as PAs. Zhao et al. [18] introduced a framework that uses PAs to infer vehicle trajectories at intersections by comparing predicted and concatenated paths. However, this approach does not account for pedestrians or cyclists, whose behavior patterns differ significantly. Zhong et al. [19] extended this concept by incorporating probabilistic models that estimate PA existence based on occlusion duration and proximity to the ego vehicle (EV).

Sequential reasoning further enhances occlusion-aware planning by dynamically eliminating unrealistic obstacle states [5], [6]. This methodology integrates reachable set analysis with motion prediction. Risk-aware motion planning, on the other hand, focuses on estimating potential dangers posed by occluded traffic participants. This approach is particularly relevant in urban scenarios involving pedestrians, aiming to minimize collisions or potential harm [20]–[22].

Building on these concepts, our earlier work [4] proposed an algorithm that integrates PA modeling with criticality metrics to assess potential risks from occluded areas. By dynamically evaluating trajectory safety and incorporating modular integration into motion planning algorithms, this approach demonstrated significant improvements in balancing proactive safety and traffic efficiency.

While the presented approaches address individual aspects of occlusion-aware planning, their isolated application is insufficient for comprehensive safety in urban environments. Reachability-based methods lack the ability to distinguish between different traffic participants, such as pedestrians, cyclists, and vehicles, in terms of their motion dynamics and associated collision risks. Conversely, agent-centric approaches often overlook the geometric feasibility of occluded areas.

III. METHODOLOGY

The limitations of existing approaches, as outlined, highlight the need for an integrated solution that combines the strengths of reachability-based and agent-centric methods. We, therefore, extend the open-source framework from our earlier work [4]. Our new approach enhances the algorithm by dynamically tracking visible areas [5], [6] to ensure PAs are placed only in critical occluded areas, extending predictions for previously visible objects, and integrating risk assessments tailored to diverse road user dynamics.

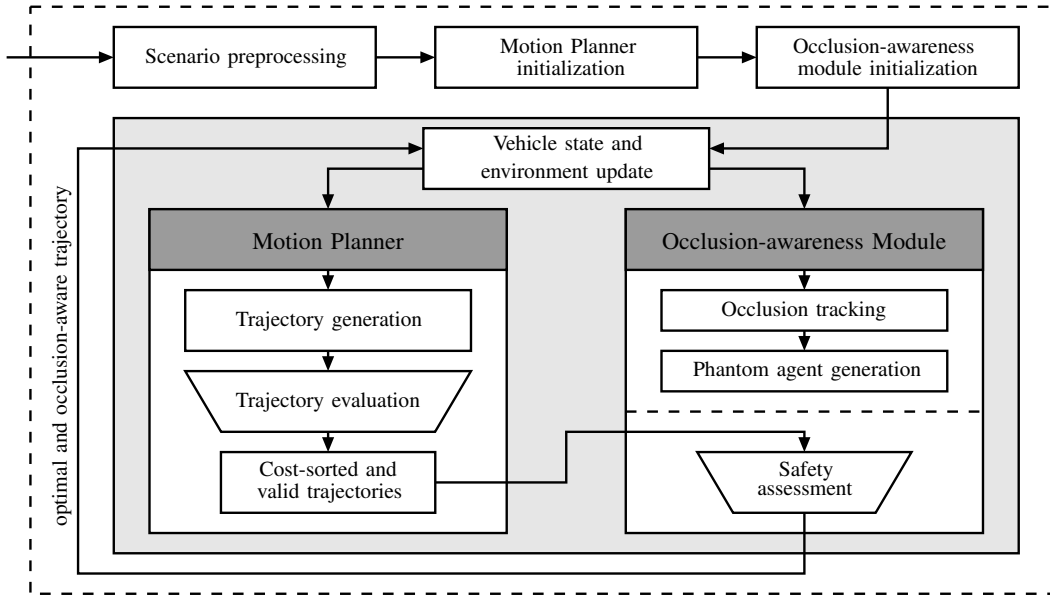


Fig. 2. Overview of the framework integrating a motion planner with our occlusion-awareness module. The motion planner generates and evaluates trajectories, providing cost-sorted and valid trajectories. The occlusion-awareness module identifies potential risks in occluded areas $\mathcal{A}_o^{\mathcal{L}}$ and performs a safety assessment. This ensures that an optimal and occlusion-aware trajectory is selected.

A. Overview of the Proposed Methodology

The proposed algorithm is designed as a modular evaluation layer that operates with existing motion planning algorithms, as shown in Figure 2. It evaluates candidate trajectories generated by the planner with respect to safety in occluded areas. To achieve this, specific information about the environment, the EV, and surrounding traffic participants is required.

The trajectories to be evaluated must be provided in global (x, y) coordinates as a time-parameterized sequence:

$$\xi(t) = \{(x_1, y_1, v_1)^\xi, (x_2, y_2, v_2)^\xi, \dots, (x_n, y_n, v_n)^\xi\}, \quad (1)$$

where v_i represents the velocity at each position (x_i, y_i) . Additionally, a global reference path Γ is required to assess the relevance of occluded areas along the planned route:

$$\Gamma = \{(x_1, y_1)^\Gamma, (x_2, y_2)^\Gamma, \dots, (x_m, y_m)^\Gamma\}. \quad (2)$$

The state of the EV and other traffic participants is defined by their global position (x, y) , orientation θ and velocity v as well as the progress s along and the lateral deviation d from Γ :

$$\mathbf{X} = [x, y, \theta, v, s, d]^\top. \quad (3)$$

The road network \mathcal{L} is modeled as a set of lanelets ℓ [23], where each lanelet $\ell_i \in \mathcal{L}$ is defined by its left boundary \mathbf{b}_l , right boundary \mathbf{b}_r , and a set of constraints \mathcal{C}^ℓ :

$$\ell_i = \{\mathbf{b}_l, \mathbf{b}_r, \mathcal{C}^\ell\}. \quad (4)$$

The boundaries \mathbf{b}_l and \mathbf{b}_r are represented as sequences of points:

$$\mathbf{b} = \{(x_1, y_1)^\mathbf{b}, (x_2, y_2)^\mathbf{b}, \dots\}. \quad (5)$$

Each lanelet ℓ_i includes specific constraints \mathcal{C}^ℓ , such as the road type (e.g., urban, highway) and maximum permissible

velocity v_{\max} . To define valid positions within a lanelet, we introduce the set $\mathcal{X}^\ell \subset \mathbb{R}^2$, which contains all points that belong to the lanelet ℓ . From \mathcal{X}^ℓ , we define the set of valid states \mathcal{X}_v^ℓ , which respect all constraints \mathcal{C}^ℓ associated with the lanelet:

$$\mathcal{X}_v^\ell = \{x \in \mathcal{X}^\ell \mid x \in \mathcal{C}^\ell\}. \quad (6)$$

These valid states \mathcal{X}_v^ℓ are critical for applications such as tracking occluded areas, as they ensure that the movement within the lanelet complies with the defined constraints, including the maximum permissible velocity v_{\max} .

By combining the EV's state, the positions of surrounding traffic participants, and the structured road network, the framework dynamically identifies occluded areas, evaluates their relevance to the planned trajectory, and assesses the safety of candidate motion plans.

B. Visible Area Calculation and Occlusion Tracking

The visible area $\mathcal{A}_v^{\mathcal{L}} \subset \mathbb{R}^2$ is required for identifying and updating occluded areas in the environment. It is computed at every timestep t ($\Delta t = 0.1$ s) based on the EV's state \mathbf{X}_{EV} and the surrounding environment, including obstacles \mathcal{O} and the road network \mathcal{L} , as shown in Algorithm 1. $\mathcal{A}_v^{\mathcal{L}}$ is defined as the region within the sensor's range \mathcal{A}_r , restricted to the area of the road network $\mathcal{A}_{\mathcal{L}}$, excluding regions occluded by obstacles:

$$\mathcal{A}_v^{\mathcal{L}} = (\mathcal{A}_r \cap \mathcal{A}_{\mathcal{L}}) \setminus \bigcup_{o \in \mathcal{O}} \mathcal{A}_o^o, \quad (7)$$

where \mathcal{A}_o^o represents the shadow area of an obstacle $o \in \mathcal{O}$, determined by the obstacle's geometry and its relative position to the EV.

Based on $\mathcal{A}_v^{\mathcal{L}}$, sequential reasoning is deployed to track and update occluded areas $\mathcal{A}_o^{\mathcal{L}}$ in the environment. The process is outlined in Algorithm 2. At the initial timestep

Algorithm 1: Visible Area and Obstacle Detection

Input : Ego Vehicle State \mathbf{X}_{EV} , Obstacles \mathcal{O} , RoadNetwork \mathcal{L} , Sensor Range \mathcal{A}_r **Output**: Visible Area $\mathcal{A}_v^{\mathcal{L}}$, Visible Obstacles \mathcal{O}_v

```
1  $\mathcal{A}_v^{\mathcal{L}} \leftarrow \text{computeRoadArea}(\mathbf{X}_{EV}, \mathcal{A}_r, \mathcal{L})$ 
2  $\mathcal{A}_v^{\mathcal{L}} \leftarrow \text{subtractObstacleShadows}(\mathcal{A}_v^{\mathcal{L}}, \mathcal{O})$ 
3  $\mathcal{O}_v \leftarrow \{\}$ 
4 foreach  $o \in \mathcal{O}$  do
5   if  $o.\text{polygon} \cap \mathcal{A}_v^{\mathcal{L}} \neq \emptyset$  then
6      $\mathcal{O}_v \leftarrow \mathcal{O}_v \cup \{o\}$ 
7   end
8 end
9 return  $\mathcal{A}_v^{\mathcal{L}}, \mathcal{O}_v$ 
```

Algorithm 2: Occlusion Tracking and Update

Input : Visible Area $\mathcal{A}_v^{\mathcal{L}}$, Road Network \mathcal{L} **Output**: Updated Occluded Area $\mathcal{A}_o^{\mathcal{L}}$

```
1 foreach  $\ell \in \mathcal{L}$  do
2   if  $\mathcal{A}_o^{\ell} = \emptyset$  then
3      $\mathcal{A}_o^{\ell} \leftarrow \text{initOcclusions}(\mathcal{A}_v^{\mathcal{L}}, \mathcal{X}_v^{\ell})$ 
4   else
5      $\mathcal{A}_o^{\ell} \leftarrow \text{expandOcclusion}(\mathcal{A}_o^{\ell}, \mathcal{X}_v^{\ell}, \mathcal{C}^{\ell})$ 
6      $\mathcal{A}_o^{\ell} \leftarrow \mathcal{A}_o^{\ell} \setminus \mathcal{A}_v^{\mathcal{L}}$ 
7   end
8 end
9 return  $\mathcal{A}_o^{\mathcal{L}} \leftarrow \bigcup_{\ell \in \mathcal{L}} \mathcal{A}_o^{\ell}$ 
```

$t_0 = 0$, when no prior observations are available, the occluded area \mathcal{A}_o^{ℓ} of a lane ℓ is determined by the valid states \mathcal{X}_v^{ℓ} of the lane that lie outside the visible area \mathcal{A}_v^{ℓ} :

$$\mathcal{A}_o^{\ell} = \{x \in \mathcal{X}_v^{\ell} \mid x \notin \mathcal{A}_v^{\ell}\}. \quad (8)$$

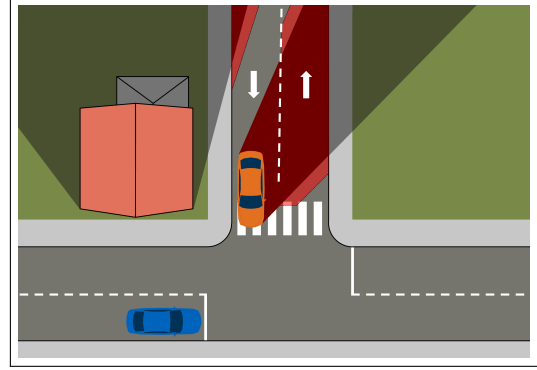
This initialization captures all areas within the lane ℓ that are not visible at t_0 , and the total occluded area is given by the union of all initial lane occlusions:

$$\mathcal{A}_o^{\mathcal{L}} = \bigcup_{\ell \in \mathcal{L}} \mathcal{A}_o^{\ell}. \quad (9)$$

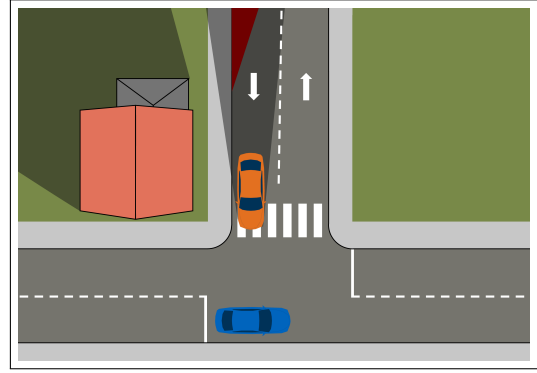
For subsequent updates, the occluded areas \mathcal{A}_o^{ℓ} are individually propagated using a point-mass motion model, which projects the previously occluded states into the future based on the motion constraints \mathcal{C}^{ℓ} . This projection captures the potential movement of hidden agents while ensuring that their dynamics remain valid within the lane's state space \mathcal{X}_v^{ℓ} . After propagation, only those projected states that remain outside the visible area \mathcal{A}_v^{ℓ} are retained as part of the updated occluded area. The updated occluded area for a lane ℓ at a given timestep is thus computed as:

$$\mathcal{A}_o^{\ell} = \left\{ x' \mid \begin{array}{l} x' = f(x, \mathcal{C}^{\ell}), x \in \mathcal{A}_o^{\ell}, \\ x' \in \mathcal{X}_v^{\ell}, x' \notin \mathcal{A}_v^{\ell} \end{array} \right\}, \quad (10)$$

ego vehicle dynamic obstacle $\mathcal{A}_o^{\mathcal{L}}$ propagated $\mathcal{A}_o^{\mathcal{L}}$



(a) Scenario at the initial timestep without prior sensor updates.



(b) Sensor measurements update the propagated occlusions, refining the occluded areas \mathcal{A}_o^{ℓ} .

Fig. 3. Illustration of an exemplary occlusion tracking process for multiple lanes $\ell \in \mathcal{L}$ at two timesteps. The visible area $\mathcal{A}_v^{\mathcal{L}}$ is shown alongside the occluded areas \mathcal{A}_o^{ℓ} (dark red) and their future propagation (light red). Grey shading represents currently unseen areas.

where $x' = f(x, \mathcal{C}^{\ell})$ denotes the projected state of a point mass $x \in \mathcal{A}_o^{\ell}$ after propagation according to \mathcal{C}^{ℓ} . For vehicle lanes, the occluded areas are expanded only in the direction of permitted traffic flow, while on sidewalks, the occluded areas are allowed to expand bidirectionally along the path to reflect pedestrian movement. After propagating the occlusions for each lane, the overall occluded area $\mathcal{A}_o^{\mathcal{L}}$ is updated according to Equation (9). This process is illustrated in Figure 3, which visualizes the propagation of exemplary occluded areas.

C. Object Prediction and Tracking

The tracking of previously visible obstacles \mathcal{O}_v is another aspect of the proposed occlusion-awareness module, ensuring that real obstacles are consistently represented, even when they temporarily leave $\mathcal{A}_v^{\mathcal{L}}$, as proposed by [17]. For faster road users like vehicles and cyclists, future states are predicted using Wale-Net [24], a neural network-based model trained to infer upcoming states based on observed movement patterns. In contrast, pedestrian states are estimated using a constant velocity approach, which assumes linear motion over the prediction horizon based on their current state.

Predictions of future positions involve uncertainty, as the motion of obstacles cannot be precisely determined. Typically, predictions are corrected at each timestep through measurement updates, which provide new information about the obstacle's state. In the case of tracking previously visible obstacles \mathcal{O}_v that have exited $\mathcal{A}_v^{\mathcal{L}}$, the uncertainty grows more significantly. Without further sensor updates, even the currently assumed state of the obstacle becomes increasingly uncertain over time.

The uncertainty is mathematically modeled using a bivariate normal distribution, which accounts for the positional variance in both the x - and y -coordinates. Formally, the predicted state \mathbf{X}_{pred} of an occluded obstacle o at time t is represented as:

$$\mathbf{X}_{\text{pred}}(t) \sim \mathcal{N}(\mu(t), \Sigma(t)), \quad (11)$$

where $\mu(t)$ is the mean position of the predicted state, and $\Sigma(t)$ is the covariance matrix describing the uncertainty, which increases over time t .

Tracking obstacles, even under growing uncertainty, ensures that the occlusion-aware motion planner anticipates their potential reappearance, reducing the risk of being unprepared for their return. If an obstacle remains unobserved for a predefined duration, it is removed from the tracked obstacles.

D. Phantom Agent Generation and Prediction Evaluation

The generation of PAs builds on the spawn point creation process proposed in [4], extending it to allow for more flexible spawn point placement and the inclusion of diverse speed and acceleration profiles. PAs are generated to represent potential road users in occluded areas $\mathcal{A}_o^{\mathcal{L}}$ identified during occlusion tracking.

Spawn points \mathcal{X}_{SP} are identified within $\mathcal{A}_o^{\mathcal{L}}$. A spawn point $x_{\text{SP}} \in \mathcal{X}_{\text{SP}}$ is considered valid if it lies within occluded area $\mathcal{A}_o^{\mathcal{L}}$ and does not intersect visible obstacles \mathcal{O}_v :

$$\mathcal{X}_{\text{SP}} = \{x_{\text{SP}} \mid x_{\text{SP}} \in \mathcal{A}_o^{\mathcal{L}} \wedge x_{\text{SP}} \notin \mathcal{O}_v\}. \quad (12)$$

For pedestrians, static spawn points are placed behind static obstacles (e.g., buildings, parked vehicles) where occlusions are most critical. The algorithm assumes a worst-case prediction where pedestrians move directly toward Γ .

Dynamic spawn points $\mathcal{X}_{\text{SP}}^{\text{dyn}}$ for cyclists and vehicles are identified in occluded areas $\mathcal{A}_o^{\mathcal{L}}$ near Γ . These points are further filtered to include only locations where potential paths γ may intersect with the EV's driving corridor:

$$\mathcal{X}_{\text{SP}}^{\text{dyn}} = \{x_{\text{SP}} \mid x_{\text{SP}} \in \mathcal{A}_o^{\mathcal{L}} \wedge \gamma(x_{\text{SP}}) \cap \Gamma \neq \emptyset\}. \quad (13)$$

For each spawn point $x_{\text{SP}} \in \mathcal{X}_{\text{SP}}$, multiple predictions are generated to account for the diverse dynamics of different road users. Each prediction is expressed as:

$$\mathbf{X}_{\text{pred}}(t) = f(x_{\text{SP}}, v, a, t), \quad t \in [t_0, t_0 + T_{\text{pred}}], \quad (14)$$

where x_{SP} is the spawn point, v the initial speed, a the acceleration (or deceleration), and T_{pred} the prediction horizon.

These predictions are subsequently used in the trajectory safety assessment step. This step is based on the approach

proposed in [4], with a particular focus on evaluating collision risks and potential damage. The explicit consideration of differing PA characteristics (e.g., VRU vs. non-VRU) allows for a nuanced risk assessment that goes beyond simple metrics such as time-to-collision (TTC). For instance, while TTC focuses solely on the temporal aspect of a potential collision, it does not account for the varying severity of a collision depending on the type of road user involved.

While our method does not guarantee complete collision avoidance, it ensures a balance between safety and efficiency. Overly conservative behavior, such as assuming every occluded area is fully occupied by worst-case scenarios, is avoided. Instead, the occlusion-awareness module evaluates the generated predictions to prioritize responses based on the likelihood and severity of potential collisions.

IV. RESULTS & ANALYSIS

Our proposed methodology is evaluated in the 2D simulation environment CommonRoad [25], using an open-source motion planner [26]. The planner generates multiple trajectory samples, selecting the optimal trajectory based on weighted cost functions. Our occlusion-awareness module is integrated to extend the planner by incorporating an additional safety assessment step, as shown in Figure 2.

Evaluation scenarios focus on conditions where real-world accidents frequently occur, such as intersections with obstructed visibility [27], [28]. The velocity profiles, risk progression, and total occluded areas $\mathcal{A}_o^{\mathcal{L}}$ are analyzed to demonstrate the benefits of our approach.

A. Velocity and Acceleration Profiles with Obstacle Tracking

Figure 4 presents the velocity and acceleration profiles for an intersection scenario where a vehicle becomes occluded for a period of time (shaded area). An exemplary situation marks a scenario, where a vehicle is temporarily hidden behind a static obstacle, such as a building. The comparison highlights two cases: one where the occluded vehicle is continuously tracked and one where it is not. In the tracking case, the occlusion-aware motion planner

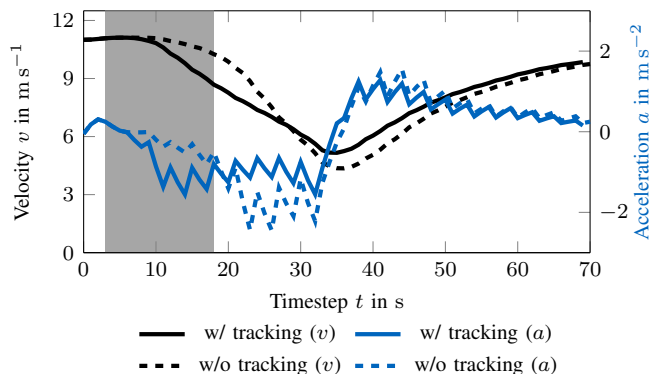


Fig. 4. Velocity and acceleration profiles for a scenario where another vehicle is occluded for a period of time (shaded area). The plot illustrates the differences in profiles when the occluded vehicle is tracked versus when it is not tracked during the occlusion period.

anticipates the reappearance of the occluded vehicle and

begins decelerating earlier—before the vehicle becomes visible again. This proactive adjustment leads to smoother velocity and acceleration profiles. In contrast, when tracking is disabled, the planner reacts only after the vehicle re-enters the visible area, resulting in abrupt deceleration and a lower minimum velocity as both vehicles are already closer to the intersection. Similar to findings in [17], tracking leads to more consistent trajectories with fewer abrupt decisions. Additionally, safety is improved, as tracking ensures greater separation from the other vehicle and allows the EV to approach the intersection at a lower, more controllable speed, leaving it better prepared to stop if necessary.

B. Qualitative Analysis of a T-Junction Scenario

In the T-junction scenario depicted in Figure 5, a stationary truck blocks the view into the intersection, creating persistent occlusions. PAs are placed in critical areas, such

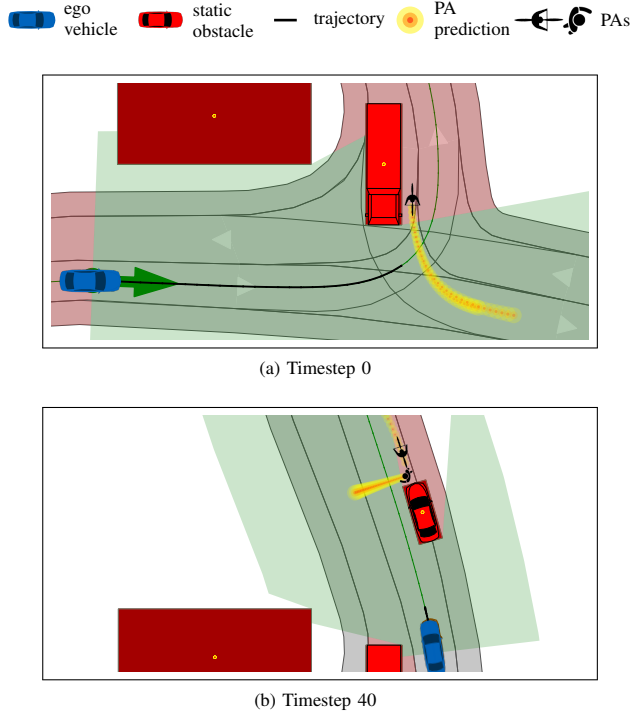


Fig. 5. Visualization of a T-junction scenario with occlusion-aware planning. The stationary truck and the parked car create persistent occlusions. PAs are generated in critical areas.

as behind the truck and along paths that intersect with the EV’s planned trajectory. Their predictions, including selected speed profiles, are visualized to highlight the safety-relevant agents. For clarity, not all generated profiles are displayed. This scenario serves as a foundation for further analyses in the following sections.

C. Sensitivity Analysis of Risk Thresholds

To evaluate the influence of the risk threshold R_{\max} on the planner’s behavior, a sensitivity analysis is conducted. The threshold is varied between $R_{\max} = 0.05$ and $R_{\max} = 0.20$, alongside an unrestricted planner ($R_{\max} = \infty$). Figure 6 visualizes velocity and respective risk profiles across the

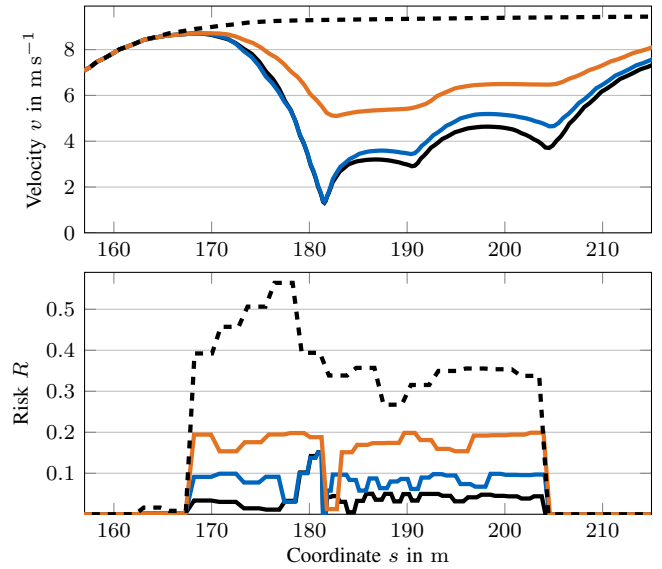


Fig. 6. Velocity and risk profiles for the T-junction scenario across four simulation runs with different risk thresholds R_{\max} .

scenario progression. Lower thresholds (stricter risk limits) lead to greater reductions in velocity to ensure compliance with the specified risk levels. This behavior is particularly evident during the turning maneuver at the T-junction, where the EV significantly slows down ($s = 181$ m). In contrast, when passing the parked vehicle, less deceleration occurs due to the lower criticality of the situation ($s = 204$ m).

An exception is observed at $s = 180$ m, where the maximum risk for $R_{\max} \leq 0.10$ is briefly exceeded. This occurs because no other valid trajectory was available. The results show the planner’s ability to adapt its behavior based on specified thresholds.

D. Comparison of our Module with Other Approaches

The performance of our proposed occlusion-awareness module is evaluated against three other approaches: a baseline planner without occlusion-awareness capabilities [26], the occlusion-aware planner from [4], and an omniscient planner with complete environmental knowledge. The T-junction scenario (see Figure 5) is used for this comparison, with a real cyclist replacing the phantom cyclist at the position shown in Figure 5a. This cyclist remains occluded by the truck until it becomes visible later in the scenario.

Velocity and risk profiles across the scenario progression are analyzed, as shown in Fig. 7. For the baseline and [4] planners, deceleration occurs only after the object becomes visible (dotted line), leading to a situation where the EV cannot brake in time due to its high speed. In contrast, our proposed method behaves similarly to the omniscient planner by decelerating proactively before the object is visible.

In the later stages of the scenario (see Figure 5b), our approach keeps a lower speed in $s = 185$ m to 200 m because potential risks are identified behind the truck and the parked vehicle, where a pedestrian or cyclist could emerge. This

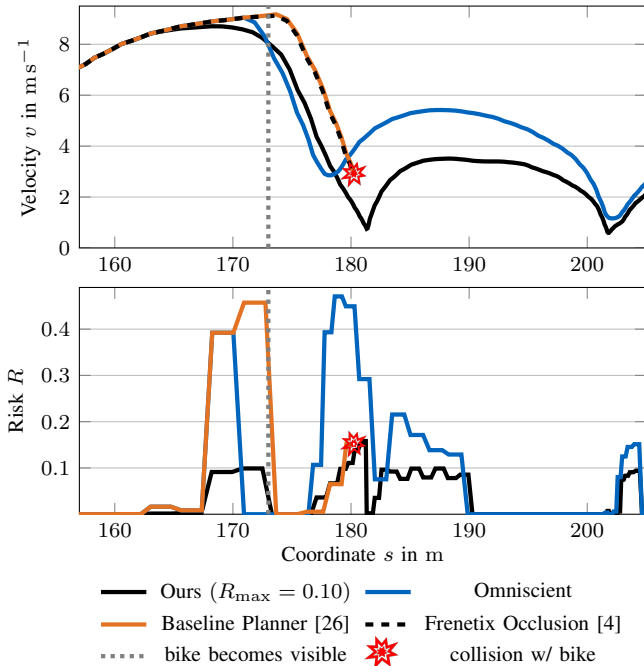


Fig. 7. Velocity and risk profiles for the T-junction scenario with a real cyclist emerging from an occlusion behind the truck, comparing different planning approaches. The dotted line marks the point at which the cyclist becomes visible.

behavior is not observed in the omniscient planner, which has complete knowledge that no such object exists in these occluded areas.

The results demonstrate that the inclusion of PAs and dynamically generated spawn points effectively addresses potential risks from occluded areas $\mathcal{A}_o^{\mathcal{L}}$.

E. Impact of Occlusion Tracking on PA Generation

A qualitative analysis of the occlusion tracking impact is shown in Figure 8, where areas that were previously visible and determined to be free of obstacles are excluded from $\mathcal{A}_o^{\mathcal{L}}$. These areas, depicted without the red occlusion overlay, pose no risk and do not generate PAs.

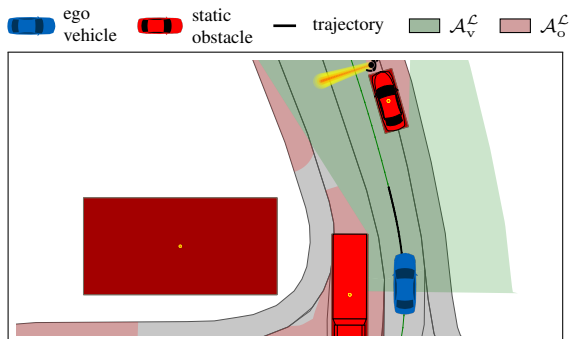


Fig. 8. Visualization of the occlusion tracking impact. Previously visible areas, determined to be obstacle-free, are excluded from the occluded area $\mathcal{A}_o^{\mathcal{L}}$, preventing unnecessary PA generation.

To quantitatively assess the effect of tracking, Figure 9 compares the evolution of $\mathcal{A}_o^{\mathcal{L}}$ in the T-junction scenario with and without occlusion tracking. The tracked case results in a

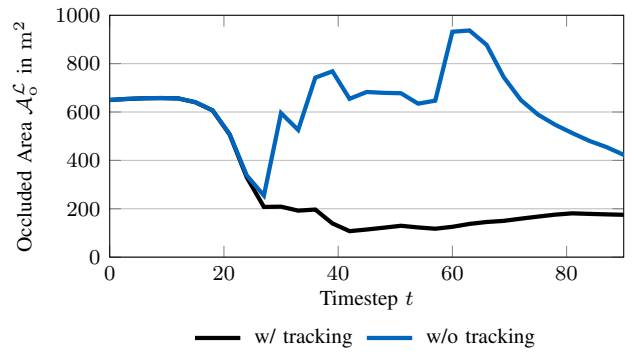


Fig. 9. Comparison of the total occluded area $\mathcal{A}_o^{\mathcal{L}}$ over time with and without occlusion tracking for the T-junction scenario. Unlike the baseline method (w/o tracking), which assumes that large areas could suddenly be occupied, our method (w/ tracking) concludes that only a part of the area is potentially occupied.

substantially smaller occluded area throughout the scenario, as previously visible areas are excluded from further consideration. Compared to the approach in [4], our method focuses more accurately on relevant occluded areas.

Finally, the aggregated effect of occlusion tracking is evaluated across seven selected CommonRoad [25] scenarios, summarized in Table I. The cumulative occluded area $\mathcal{A}_o^{\mathcal{L}}$ is

TABLE I
REDUCTION OF $\mathcal{A}_o^{\mathcal{L}}$ WITH OCCLUSION TRACKING (OT)

Scenario	$\sum \mathcal{A}_o^{\mathcal{L}}$ (OT)	$\sum \mathcal{A}_o^{\mathcal{L}}$	Reduction
1	7961.7 m ²	11 953.8 m ²	33.40 %
2	2780.8 m ²	4759.1 m ²	41.57 %
3	2661.7 m ²	2744.5 m ²	3.02 %
4	1115.1 m ²	1861.7 m ²	40.10 %
5	1326.9 m ²	2880.5 m ²	53.94 %
6	987.7 m ²	1659.7 m ²	40.49 %
7	2308.7 m ²	3446.0 m ²	33.00 %

computed over the scenario duration, both with and without tracking. Particularly in scenarios involving intersections, occlusion tracking (OT) achieves an $\mathcal{A}_o^{\mathcal{L}}$ reduction of up to 54%. This demonstrates that tracking enables the planner to focus on critical areas.

V. DISCUSSION

The simulation results highlight how our proposed method enables safer navigation in urban environments with occlusions. By combining occlusion tracking with PA generation, our approach addresses occluded areas while avoiding overly conservative behavior. A key advancement over [4] lies in the targeted placement of PAs. Instead of considering all occluded areas, PAs are generated only in areas deemed critical to the EV's planned trajectory. This focused approach reduces unnecessary complexity while allowing a more detailed safety assessment for high-risk areas. By incorporating multiple speed and acceleration profiles, the algorithm further ensures that a wide range of potential agent behaviors is accounted for.

The evaluation scenarios were carefully selected to replicate real-world accident-prone situations. However, additional tests across more diverse environments remain necessary to validate generalizability. Moreover, the selection of criticality thresholds remains a challenging aspect. A key limitation of the current implementation lies in its computational efficiency. It is not yet optimized for real-time deployment on a real-world vehicle. Specifically, the sequential trajectory evaluation during safety assessment can result in significant computational overhead, particularly in complex scenarios with numerous occlusions and high PA densities.

VI. CONCLUSION & OUTLOOK

This work presents an integrated occlusion-aware planning algorithm that advances the state of the art in AV motion planning. By combining sequential occlusion tracking with PA generation, our approach addresses the challenge of navigating occluded environments. The proposed methodology improves upon previous methods such as [4] by incorporating multiple speed and behavior profiles, enabling a more nuanced evaluation of potential hazards. Simulations demonstrate the methods's ability to react proactively to occluded areas while avoiding overly conservative behavior.

Despite its promising results, the current implementation serves as a proof of concept and requires further refinement for deployment in real-world vehicles. First, the Python-based implementation must be re-engineered into a more efficient language, such as C++, to achieve real-time performance. Second, the sequential safety assessment process should be integrated into the motion planning pipeline itself. By discarding infeasible trajectories during the trajectory generation phase, computational costs can be significantly reduced, and responsiveness improved.

Future work will also focus on validating the method in real-world scenarios using a real vehicle. Furthermore, expanding the framework to include richer traffic rules and environmental constraints could improve performance, particularly in complex urban settings. These enhancements, combined with broader testing in diverse scenarios, will ensure the method's robustness and practical applicability.

REFERENCES

- [1] A. Herrmann, W. Brenner, and R. Stadler, *Autonomous Driving: How the Driverless Revolution Will Change the World*. Emerald Publishing Limited, Mar. 2018.
- [2] K. Yang, X. Tang, J. Li, H. Wang, G. Zhong, J. Chen, and D. Cao, "Uncertainties in onboard algorithms for autonomous vehicles: Challenges, mitigation, and perspectives," *IEEE Transactions on Intelligent Transportation Systems*, vol. 24, no. 9, Sep. 2023.
- [3] S. Singh, "Critical reasons for crashes investigated in the national motor vehicle crash causation survey," Washington, DC, 2018.
- [4] K. Moller, R. Trauth, and J. Betz, "Overcoming blind spots: Occlusion considerations for improved autonomous driving safety," in *IEEE Intelligent Vehicles Symposium (IV)*, Jun. 2024.
- [5] L. Wang, C. Burger, and C. Stiller, "Reasoning about potential hidden traffic participants by tracking occluded areas," in *IEEE International Intelligent Transportation Systems Conference (ITSC)*, Sep. 2021.
- [6] J. M. G. Sanchez, T. Nyberg, C. Pek, J. Tumova, and M. Torngren, "Foresee the unseen: Sequential reasoning about hidden obstacles for safe driving," in *IEEE Intelligent Vehicles Symposium (IV)*, Jun. 2022.
- [7] C. Zhang, S. Ma, M. Wang, G. Hinz, and A. Knoll, "Efficient pomdp behavior planning for autonomous driving in dense urban environments using multi-step occupancy grid maps," in *IEEE International Conference on Intelligent Transportation Systems (ITSC)*, 2022.
- [8] K. H. Wray, B. Lange, A. Jamgochian, S. J. Witwicki, A. Kobashi, S. Hagaribommanahalli, and D. Ilstrup, "Pomdps for safe visibility reasoning in autonomous vehicles," in *IEEE International Conference on Intelligence and Safety for Robotics (ISR)*. IEEE, 2021.
- [9] M. Koschi and M. Althoff, "Set-based prediction of traffic participants considering occlusions and traffic rules," *IEEE Transactions on Intelligent Vehicles*, vol. 6, no. 2, 2021.
- [10] P. F. Orzechowski, A. Meyer, and M. Lauer, "Tackling occlusions & limited sensor range with set-based safety verification," in *International Conference on Intelligent Transportation Systems (ITSC)*. IEEE, 2018.
- [11] S. Lee, W. Lim, M. Sunwoo, and K. Jo, "Limited visibility aware motion planning for autonomous valet parking using reachable set estimation," *Sensors*, vol. 21, no. 4, Feb. 2021.
- [12] B. Gilhuly, A. Sadeghi, P. Yedemellat, K. Rezaee, and S. L. Smith, "Looking for trouble: Informative planning for safe trajectories with occlusions," in *International Conference on Robotics and Automation (ICRA)*, 2022.
- [13] P. Narksri, H. Darweesh, E. Takeuchi, Y. Ninomiya, and K. Takeda, "Occlusion-aware motion planning with visibility maximization via active lateral position adjustment," *IEEE Access*, vol. 10, 2022.
- [14] T. de Borja, O. Vaculín, H. Marzbani, and R. N. Jazar, "Increasing safety of vulnerable road users in scenarios with occlusion: A collaborative approach for smart infrastructures and automated vehicles," *IEEE Access*, vol. 13, 2025.
- [15] T. Nyberg, J. M. G. Sánchez, V. Narri, H. Pettersson, J. Mårtensson, K. H. Johansson, M. Törngren, and J. Tumova, "Share the unseen: Sequential reasoning about occlusions using vehicle-to-everything technology," *IEEE Transactions on Control Systems Technology*, 2024.
- [16] V. Trentin, J. Medina-Lee, A. Artuñedo, and J. Villagra, "Integrating occlusion awareness in urban motion prediction for enhanced autonomous vehicle navigation," in *IEEE Intelligent Vehicles Symposium (IV)*, 2024.
- [17] Z. Pang, D. Ramanan, M. Li, and Y.-X. Wang, "Streaming motion forecasting for autonomous driving," in *IEEE/RSJ International Conference on Intelligent Robots and Systems (IROS)*, 2023.
- [18] X. Zhao, C. Zhang, J. Wang, and Y. Zhu, "Inference and planning at occluded intersections for urban autonomous driving," *IEEE Transactions on Intelligent Vehicles*, 2024.
- [19] Y. Zhong and H. Peng, "Driving with caution about fully occluded areas based on occupancy maps," in *IEEE International Conference on Intelligent Transportation Systems (ITSC)*, 2023.
- [20] D. Wang, W. Fu, J. Zhou, and Q. Song, "Occlusion-aware motion planning for autonomous driving," *IEEE Access*, vol. 11, 2023.
- [21] M. Koc, E. Yurtsever, K. Redmill, and U. Oezgüner, "Pedestrian emergence estimation and occlusion-aware risk assessment for urban autonomous driving," in *IEEE International Intelligent Transportation Systems Conference (ITSC)*, 2021.
- [22] R. Trauth, K. Moller, and J. Betz, "Toward safer autonomous vehicles: Occlusion-aware trajectory planning to minimize risky behavior," *IEEE Open Journal of Intelligent Transportation Systems*, 2023.
- [23] P. Bender, J. Ziegler, and C. Stiller, "Lanelets: Efficient map representation for autonomous driving," in *IEEE Intelligent Vehicles Symposium Proceedings*, Jun. 2014.
- [24] M. Geisslinger, P. Karle, J. Betz, and M. Lienkamp, "Watch-and-learn-net: Self-supervised online learning for probabilistic vehicle trajectory prediction," in *IEEE International Conference on Systems, Man, and Cybernetics (SMC)*, 2021.
- [25] M. Althoff, M. Koschi, and S. Manzingler, "Commonroad: Composable benchmarks for motion planning on roads," in *IEEE Intelligent Vehicles Symposium (IV)*, 2017.
- [26] R. Trauth, K. Moller, G. Würsching, and J. Betz, "Frenetix: A high-performance and modular motion planning framework for autonomous driving," *IEEE Access*, 2024.
- [27] National Highway Traffic Safety Administration and U.S. Department of Transportation, "Comparing demographic trends in vulnerable road user fatalities and the u.s. population, 1980–2019," 2021.
- [28] P. Olszewski, P. Szagała, D. Rabczenko, and A. Zielińska, "Investigating safety of vulnerable road users in selected eu countries," *Journal of Safety Research*, vol. 68, Feb. 2019.